Evaluation of multilayer defect repair viability and protection techniques for EUV masks

Takeshi Isogawa [a], Kazunori Seki [a], Mark Lawliss [b], Zhengqing John Qi [b]
Jed Rankin [b], Shinji Akima [a]

[a]Toppan Photomasks Inc., 1000 River St., Essex Junction, VT 05452, USA
[b] GLOBALFOUDRIES, 1000 River St., Essex Junction, VT 05452, USA

Phone: +1-802-769-8325 FAX: +1-802-769-5909 e-mail: takeshi.isogawa@toppan.co.jp

ABSTRACT

A variety of repairs on EUV multilayer were conducted including protection against pattern degradation in manufactural use in order to evaluate feasibility of multilayer repair and the protection schemes. The efficacy of post-repair protection techniques are evaluated to determine the lifetime of multilayer repairs. Simulations were used to select the optimal material thicknesses for repair protection, and the simulation results are verified with the lithographic results. The results showed a high correlation coefficient. Finally, all repaired sites were cleaned multiple times to quantify repair durability and impact on wafer CD. Aerial imaging of the repair sites before and after cleans shows a dramatic degradation of wafer CD post-cleaning. However, we show that applying a surface protection material after multilayer repair successfully mitigates the influence of multilayer degradation during extensive manufacturing operations.

Keywords: EUV, absorber stacks, mask defect repair, repairability, printability

1 INTRODUCTION

Mask defectivity is one of the major concerns for EUV masks. In the mask fabrication process, total mask defects represent a combination of intrinsic blank defects, and defects introduced during the mask patterning process. Intrinsic blank defects are particularly challenging because their elimination is outside of conventional repair methodologies. Past repair methodologies have utilized nanomachining of the multilayer mirror as a potential solution [1].

Nanomachining repairs involve excavating the multilayer to mitigate any coherent disruptions which come from intrinsic blank defects. However, this creates a concern by exposing the sidewall of the multilayer, which may experience structural and reflectivity degradation through mask cleaning lifetime and wafer exposure [2].

In order to prevent the degradation of these multilayer repairs, we introduce a methodology which protects the repaired sites by means of surface treatment with minimal impact to Bragg reflectivity.

2 METHODS

The EUV blank used for this study was built with the standard film structure: 60nm of absorber layer, 2.5nm of Ru-capping layer, 40 pairs of Mo/Si bi-layers on the substrate and backside film of CrN. The mask patterning processed 180nm hole arrays in order for better control of the repair proces. As an initial procedure, Figure 1 shows the repair processes. First, an

Photomask Technology 2015, edited by Naoya Hayashi, Bryan S. Kasprowicz, Proc. of SPIE
Vol. 9635, 963518 · © 2015 SPIE · CCC code: 0277-786X/15/$18 · doi: 10.1117/12.2197761

Downloaded From: http://spiedigitallibrary.org/ on 11/21/2015 Terms of Use: http://spiedigitallibrary.org/ss/TermsOfUse.aspx

electron beam (EB) repair tool was used to widening the absorber pattern, and then a nanomachining repair tool was used to excavate various amounts of multilayer. Two types of repairs were performed; type A repair excavates the whole region of the hole, type B repair excavates a partial region at the central of the hole, as shown in Figure 1. The dimensions of repair are targeted from 30nm to 90nm in the lateral direction, and from 35nm to 70nm in depth, following previous work[1].

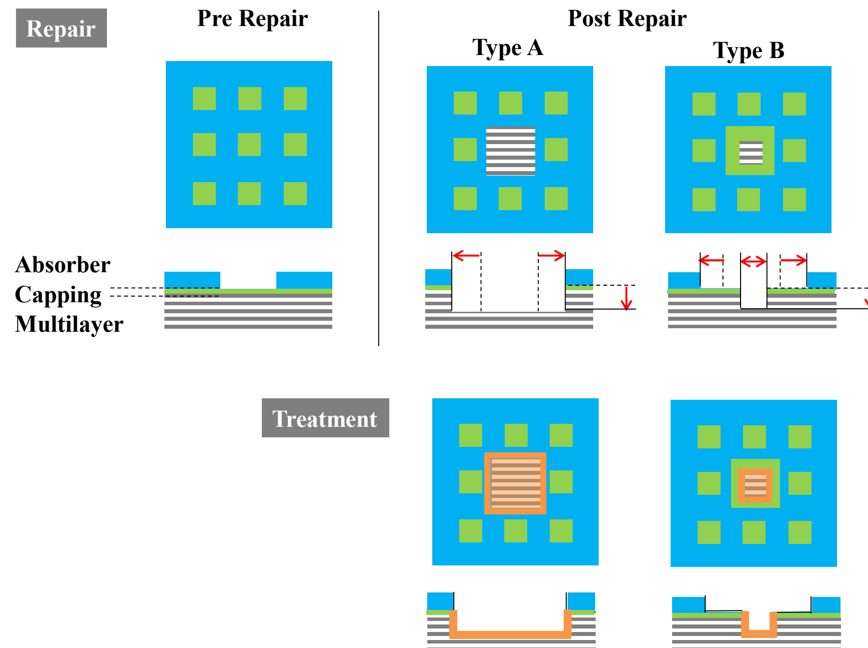

Figure 1. Process of repair and post-repair treatment

After applying the repair process to the pattern, three kinds of protective layer treatments were performed in order to quantify the efficiency of protection from multilayer degradation during cleans. Since EUV emulating tools (i.e. EUV AIMS^{TM}) is not commercially available, rigorous 3D EUV mask simulations help predict wafer printing characteristics. Figure 2 shows simulation results of the post-repair treatment's influence on wafer critical dimension (CD) change. Generally, as the post-repair protective layer treatment increases in thickness, the more change in wafer CD occurs due to the increase in absorption of EUV light from the thicker protective layer. In manufacturing operation, the thickness of post treatment must minimize wafer CD change. The treatment thickness used for our subsequent experiments is targeted to maintain imaged lithographic CD as compared to a non-treatment site. The specification was set at -5% change in wafer CD as an acceptable baseline, and the maximum thickness of each treatment was determined form this baseline. The thickness of treatment A was determined to be 6nm, treatment B is 1nm, and treatment C is 5nm. It should be noted that thicker treatments can be used if the repaired dimension is appropriately compensated.

Downloaded From: http://spiedigitallibrary.org/ on 11/21/2015 Terms of Use: http://spiedigitallibrary.org/ss/TermsOfUse.aspx

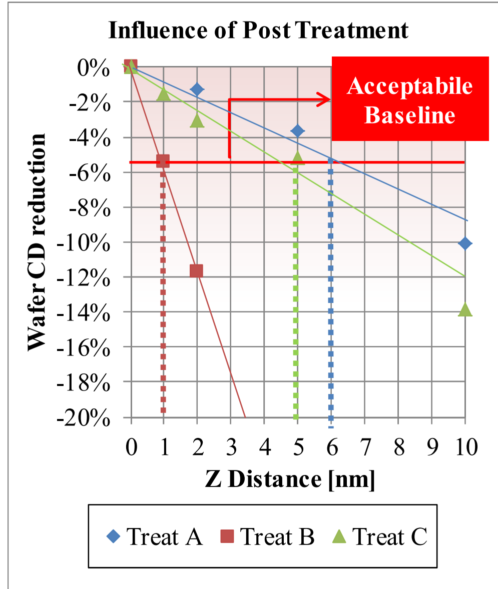

Figure 2 Simulated influence of post-repair protective layer treatment versus wafer CD change

To characterize the mask, the repaired sites were measured for CD, depth, and cross section profile by means of Scanning Electron Microscope (SEM) and Atomic Force Microscope (AFM). An EUV microscope[3] enables capturing aerial images with the same illumination setting (NA, source) as an EUV scanner. To simulate wafer printability, CD on aerial image was measured by defining a certain threshold. Measured value on the mask pattern is used for building a simulation model. Simulated wafer CD is compared to EUV microscope aerial CD in order to validate the simulation model.
The mask had multiple cleanings applied to the mask to accelerate pattern degradation, to replicate conditions a non-pellicled mask may see in normal fab operations[2]. We compared mask characteristic and wafer printability between cleanings to evaluate how much cleaning degrades the repaired sites and which treatment method is the most protective to minimize pattern degradation.

3 RESULTS AND DISCUSSIONS

3.1 Multilayer repair simulation

Figure 3 shows aerial CD correlation result between EUV microscopic image and simulation. The correlation coefficient showed more than 0.9 which illustrates high confidence in the simulated model. Therefore, it was concluded that the current simulation model is very reliable for evaluating multilayer repair and represents a valuable tool for predicting target repair geometries.

Downloaded From: http://spiedigitallibrary.org/ on 11/21/2015 Terms of Use: http://spiedigitallibrary.org/ss/TermsOfUse.aspx

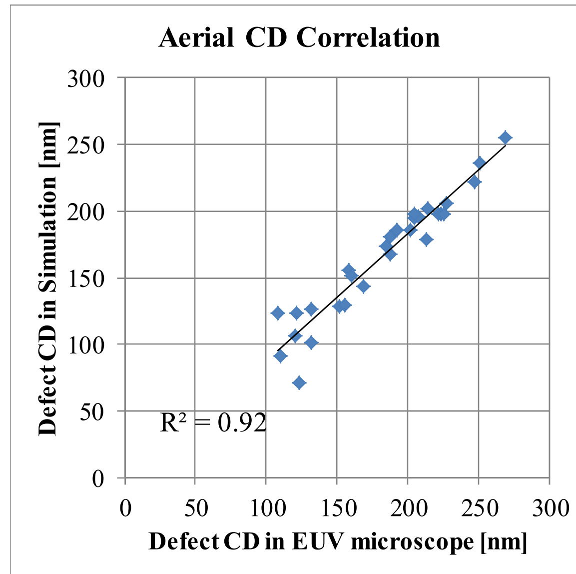

Figure 3 Correlation result of defect correlation CD between EUV microscope and simulation

3.2 Cleaning impact on multilayer

3.2.1 Repair target size dependencies

On left charts in Figure 4 show the comparison between pre- and post-cleaning characteristics in the aerial image and mask profile in order to assess cleaning impact. Aerial CD changes were measured by applying a threshold to the microscopic's aerial image. Type A repair showed 22% CD change in average and varied from 3% to 73% change depending on repaired site. Type B repair showed 12% CD change in average and varied from 4% to 22% depending on repaired site. Type A had a bigger change than type B, presumably because type A has a wider multilayer opening.

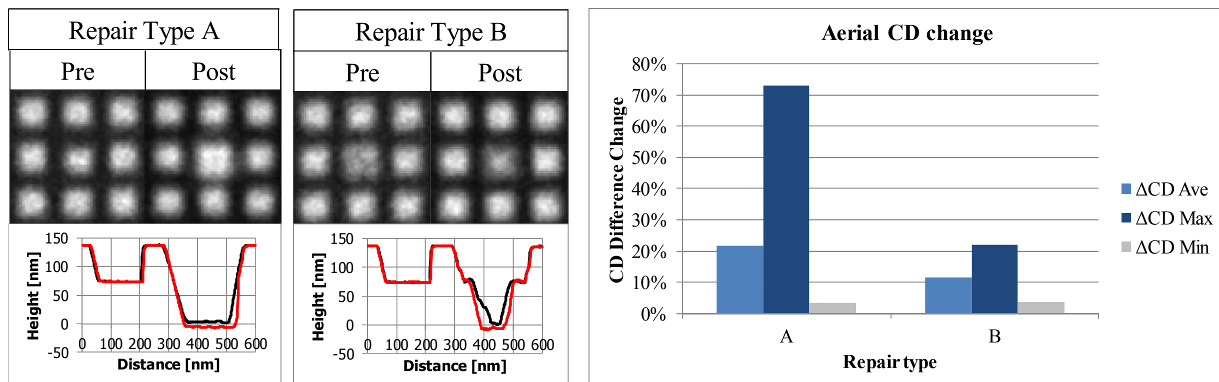

Figure 4 Characteristics change on each repair type: Cleaning changes mask pattern wider and deeper

Figure 5 shows the cleaning influences depending on repair target size for type A. Mask dimension change and aerial CD change were compared between cleanings. The result showed that as the repair target size gets bigger, the repaired site tends to be influenced more by repeated cleans. Especially, the deeper repair makes changes both for aerial CD and mask

Downloaded From: http://spiedigitallibrary.org/ on 11/21/2015 Terms of Use: http://spiedigitallibrary.org/ss/TermsOfUse.aspx

dimensions such as CD and depth. If Z equals 0 (no repair), mask depth showed no change even if multiple cleanings were applied, because the intact capping layer is designed to protect the multilayer.

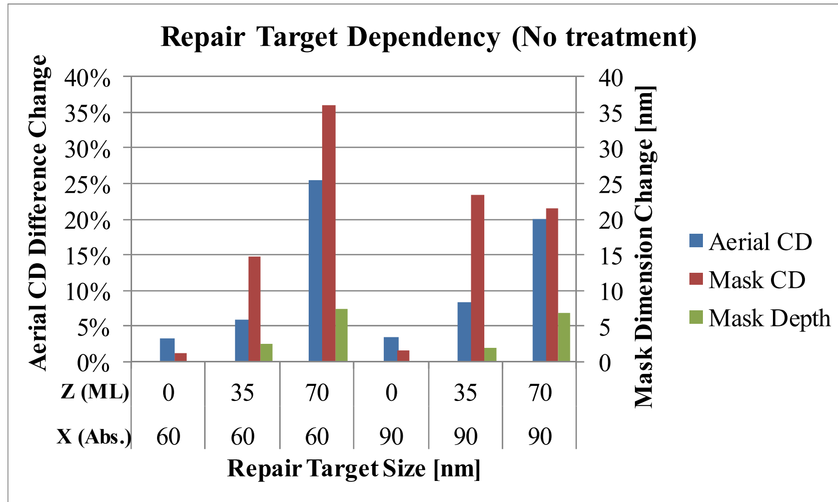

Figure 5 Repair target size dependency to cleaning influence

3.2.2 Post treatment comparison

Figure 6 shows the post repair treatment comparison results. Every treatment result captured both best-focus aerial image and in positive and negative focus. The graph in Figure 6 shows the aerial CD change through focus planes. In terms of aerial CD change between cleaning at best focus, no treatment showed 22%, treatment A showed 18%, treatment B showed 9% and treatment C showed 3%. Off-focus results of aerial CD change showed the same order of CD impact as best focus plane. No treatment after repair showed the largest amount of change after cleaning.

	None		Treat A		Treat B		Treat C	
	Pre	Post	Pre	Post	Pre	Post	Pre	Post
Minus focus								
Best focus								
Plus focus								

Downloaded From: http://spiedigitallibrary.org/ on 11/21/2015 Terms of Use: http://spiedigitallibrary.org/ss/TermsOfUse.aspx

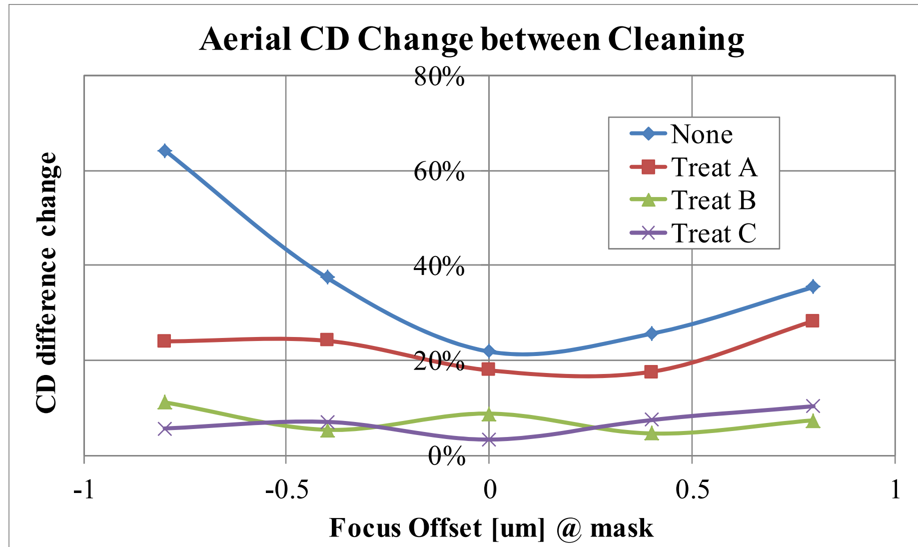

Figure 6 Post repair treatment comparison between cleaning

4 SUMMARY

A variety of repairs on EUV multilayer including protection against pattern degradation were conducted on 180nm contact holes using nanomachining and EB repair technologies. The repair target was guided by past work. Rigorous simulations were also used in order to target the amount of post-repair protective surface treatment to apply so that protected repaired sites can maintain its reflectivity. The simulation results were verified with the experimental lithographic results from an EUV microscope. Correlation coefficient between simulated and experimental aerial CD showed more than 0.9, indicating that simulations represent a promising tool to predict wafer characteristics for multilayer repair, impact of surface treatment on multilayer repair, and provide guidance on life-time degradation mitigation techniques. Durability and lifetime of multilayer repairs was tested by subjecting the repaired sites to multiple cleans and experimental aerial imaging between pre- and post-cleaning was captured. Cleaning impact on the repaired site was assessed by change in aerial CD. Type A repairs, which has the entire exposed multilayer region excavated of one contact hole, showed 22% CD change post-cleaning. Type B repairs, which has the exposed multilayer excavated partially in one contact hole, showed 12% CD change post-cleaning. It was found that by applying a post-repair surface protection layer, aerial image CD degradation due to cleans was minimized to 3~9% aerial CD change as compared to repair sites with no treatment, which showed around 20% aerial CD change. Additionally, we have demonstrated that if there is an expectation that the mask may receive multiple cleanings after fabrication, there may be significant degradation on any repairs penetrating the capping layer into the multilayer stack.

ACKNOWLEDGEMENTS

The authors would like to thank the following for their contributions to this paper. Kenneth Goldberg of Lawrence Berkeley National Laboratory and the SHAPR (The SEMATECH High-NA Actinic Reticle review Project) team for EUV microscope imaging, Luke Bolton and Christopher Jarvis of GLOBALFOUNDRIES for mask repairing, Christina A Turley and Louis Kindt of GLOBALFOUNDRIES for mask cleaning, Peter Bartlau and Michael Hibbs of GLOBALFOUNDRIES for mask handling. Finally we would like to thank the GLOBALFOUNDRIES and Toppan management and technical teams for support of this project.

Downloaded From: http://spiedigitallibrary.org/ on 11/21/2015 Terms of Use: http://spiedigitallibrary.org/ss/TermsOfUse.aspx

REFERENCES

[1] Lawliss, M., et al., "Repairing native defects on EUV mask blanks" Proc. SPIE 9235, 923516 (2014).

[2] Turley, C., et al., "EUV mask black border evolution" Proc. SPIE 9235, 923513 (2014).

[3] Kenneth A. Goldberg et al., "The SEMATECH high-NA actinic reticle review project (SHARP) EUV mask-imaging microscope" Proc. SPIE 8880, 88800T-1 (2013).

Downloaded From: http://spiedigitallibrary.org/ on 11/21/2015 Terms of Use: http://spiedigitallibrary.org/ss/TermsOfUse.aspx